Bimetallic Au-Cu Nanoparticles Anchored Reduced Graphene Oxide as Efficient Catalyst for Reduction of Nitro Aromatic Compounds

A Dissertation
Submitted in partial fulfilment

FOR THE DEGREE
OF
MASTER OF SCIENCE IN CHEMISTRY

Under The Academic Autonomy
NATIONAL INSTITUTE OF TECHNOLOGY, ROURKELA

By
Padmini Sahoo
413CY2016

Under the Guidance of
Dr. Priyabrat Dash

DEPARTMENT OF CHEMISTRY
NATIONAL INSTITUTE OF TECHNOLOGY
ROURKELA – 769008
ODISHA

May, 2015

CERTIFICATE

Dr.Priyabrat Dash
Assistant Professor
Department of Chemistry
NIT, Rourkela-ODISHA

This is to certify that the dissertation entitled ***"Bimetallic Au-Cu Nanoparticles Anchored Reduced Graphene Oxide as Efficient Catalyst for Reduction of Nitro Aromatic Compounds"*** *being submitted by* ***Padmini Sahoo*** *to the Department of Chemistry, National Institute of Technology, Rourkela, Odisha, for the award of the degree of Master of Science in Chemistry is a record of bonafide research work carried out by her under my supervision and guidance. I am satisfied that the dissertation report has reached the standard fulfilling the requirements of the regulations relating to the nature of the degree*.

Rourkela-769008

Date: 5th May 2015

Dr. Priyabrat Dash

(Supervisor)

ACKNOWLEDGEMENTS

First of all, I am thankful to my guide Dr. Priyabrat Dash who untiringly assisted me in my experiment and enhanced my knowledge base by making me aware about this project. My training would not have been successfully completed without the firm guidance of my guide who supervised me in all my experiments.

I like to thank all faculty members of the Department of chemistry, who have always inspire me to work hard and helped me to learn new concepts and experiments during my stay at NIT, Rourkela.

I would like to thank my parents for their unconditional love and support. They have helped me in every situation throughout my life, I am grateful for their support.

I would like to accord my sincere gratitude to Miss Lipeeka Rout for her valuable help and guidance throughout the project. Also thanks to Miss Basanti Ekka and Mr. Aniket Kumar for their valuable suggestions, guidance in carrying out experiments. Finally, I would like to thank all my labmates Jyoshna, Anurag and Pradyuman for all fun times we had together in the lab.

Finally I would like to thank all my friends for their support and the great almighty to shower his blessing on us and making dreams and aspirations.

Padmini Sahoo

ABSTRACT

In the present work an efficient nanocomposite Au-Cu/rGO has been synthesised by decorating Au-Cu bimetallic nanoparticles on reduced graphene oxide surface via co-reduction method. The nanocomposite was characterized using X-ray diffraction (XRD), Field-emission Scanning electron microscopy (FE-SEM), Energy dispersive X-ray spectroscopy (EDS), Transmission electron microscopy (TEM) and UV-Visible spectroscopy. The FE-SEM and TEM images demonstrate the uniform distribution of the Au-Cu bimetallic nanoparticles on the GO surface and transmission electron microscopy (TEM) confirms an average particle size of 6-8 nm. The Au-Cu/rGO nanocomposite has been found to be an extremely efficient catalyst for the reduction of nitroaromatic compounds into nitroamine compounds. The Au-Cu/rGO nanocomposites exhibited synergistically more superior catalytic efficiency compared to monometallic Au nanoparticles doped reduced graphene oxide and monometallic Cu nanoparticles doped reduced graphene oxide. The reaction conditions were optimized by changing different parameters such as catalyst dose and reducing agent concentration.

CONTENTS

		PAGE
CERTIFICATE		ii
ACKNOWLEDGEMENTS		iii
ABSTRACT		iv
TABLE OF CONTENTS		v-vii
LIST OF FIGURE		viii
LIST OF SCHEMES		ix
CHAPTER 1	**INTRODUCTION**	
1.1	General Introduction	1-2
1.2	Graphene	2
1.3	Graphene Oxide: Structure	3
1.4	Graphene Oxide: Properties and Application	3
1.5	Reduced Graphene Oxide	4
1.6	Nanocomposites	5
1.7	Reduced Graphene Oxide Based Nanocomposites	5
1.8	Synthesis of Reduced Graphene Oxide Based Nanocomposites	6
1.9	Approaches for Synthesis of Nanomaterials	6
1.10	Bimetallic Nanoparticles	7
1.11	Methods of Synthesis of Nanoparticles	7
1.11.1	Co-reduction Method	8
1.11.2	Sequential Reduction Method	8
1.12	Characterization Techniques	9
1.13	Reduction of Nitro Groups	9-10

1.14	Objectives	10
1.15	Importance of Our Work	11
CHAPTER 2	**EXPERIMENTAL**	
2.1	Materials	12
2.2	Synthesis	12
2.2.1	Synthesis of Reduced Graphene Oxide	12
2.2.2	Synthesis of Au-Cu Bimetallic Nanoparticles	12
2.2.3	Synthesis of Cu Doped r-GO Nanocomposite	13
2.2.4	Synthesis of Au Doped r-GO Nanocomposite	13
2.2.5	Synthesis of Au-Cu doped r-GO Nanocomposite	13
2.3	Reduction of Nitroaromatic Compounds	13
2.4.	Characterizations	13-14
CHAPTER 3	**RESULTS AND DISCUSSION**	
3.1	UV-Vis Study	15
3.2	XRD Study	16
3.3	FESEM/EDX Analysis	17
3.4	TEM/SAED Study	18-19
3.5	Catalytic Activity	20
3.5.1	Catalytic Reduction of *p*-nitroaniline and Other Nitro Aromatic Compounds	20

3.5.1.1	Catalytic Activity of Monometallic and Bimetallic NPs doped rGO	20
3.5.1.2	Effect of Catalyst Dose	21
3.5.1.3	Effect of $NaBH_4$ Concentration	22
3.5.2	Schematic Representation of Nitroaniline Reduction	23
3.5.3	Reduction of Other Nitroaromatic Compounds	25
CHAPTER 4	**CONCLUSIONS**	26
CHAPTER 5	**FUTURE WORK**	27
CHAPTER 6	**REFERENCES**	28-29

List of Figures

Fig.No		Page No.
1	A layer of grapheme.	2
2	A layer of graphene oxide.	3
3	Oxidation of graphene to graphene oxide and reduction of graphene oxide to grapheme.	4
4	Oxidation of graphene to graphene oxide and reduction of graphene oxide to reduced graphene oxide.	5
5	Top-down and bottom-up approach for nanomaterials synthesis.	6
6	Types of bimetallic nanoparticles: a) alloy nanoparticle, b) core-shell nanoparticle and c) cluster in cluster nanoparticle.	7
7	UV-Vis spectra of synthesized catalysts.	15
8	XRD pattern of synthesized catalysts.	16
9	FESEM micrograph of (a) Reduced graphene oxide, (b) Au-Cu/rGO and (c) EDX spectra of Au-Cu/rGO.	18
10	TEM image of Au-Cu/rGO	19
11	Absorption spectra of MNBA to MABA using Au-Cu/rGO catalyst.	21
12	Change in concentration for reduction of MNBA using Cu-rGO, Au-rGO and Au-Cu/rGO.	21
13	Reduction of PNA to PPDA with different catalyst dose.	22
14	Reduction of PNA to PPDA with change in $NaBH_4$ concentrations.	23
15	Schematic representation of reduction of p-nitroamine to p-phenyldiamine.	24
16	Plot showing the reduction of (a) p-nitroaniline, (b) p-nitrophenol, (c) m-nitrobenzoic acid, (d) o-nitrobenzoic acid	25

and (e) p-nitrobenzoic acid.

List of Schemes

S.No	Schemes	Page.No.
1	Schematic Representation of Co-reduction method.	8
2	Schematic Representation of the Sequential reduction method.	8
3	A general scheme for reduction of nitroarene to aminoarene.	10
4	Model reaction for reduction of MNBA to MABA using various catalysts.	21
5	Model reaction involving reduction of PNA to PPDA.	23

Chapter 1

INTRODUCTION

1.1. General Introduction

Nanoparticles are the recent and most studied topics as they exhibit interesting catalytic properties and wide applications in different fields. The nanoparticles are classified as materials having size 1-100 nm.[1] The small size of the nanoparticles results in quantum effects thus leads to high surface area to volume ratio and increase in number of surface atoms in comparison to core atoms. These properties result in very high catalytic activity.[2] These nanoparticles can be monometallic or bimetallic. Bimetallic nanoparticles are considered superior to monometallic as they have a synergistic effect of both the metals used for their synthesis. Due to their diverse properties, they are used in widespread field such as catalysis, electrochemistry, magnetism, optics, and biomedicine. These applications often highly depend on the structure like shape, size, composition, and surface chemistry of the nanoparticles.[3]

Gold and copper are two such coinage metals which are extensively used for catalysis process. They have superficially similar chemistry yet they show very different behaviour. Copper nanoparticles are considered to be very reactive as they oxidize as they come in contact with air and water. They are very good catalysts for oxidation of alcohols to aldehydes and reduction process. On the other hand, gold catalysts are used only for selective reactions and can be used in a broad range of organic transformations. Combining their properties in bimetallic nanoparticles has influenced the oxidation and reduction reactions considerably. They are found to be active catalysts used in wide range of organic transformation with high selectivity.[4]

Because of its two dimensional structure and high surface area, graphene oxide is preferred for a support system for nanoparticles. When doped with nanoparticles they show excellent catalytic property. Also they exhibit surface functionality due presence of sp^3 carbon surrounding sp^2 carbon and oxygen containing hydrophilic group.[5] Here, we have combined the properties of Au-Cu bimetallic particles with that of the graphene oxide and have observed tremendous catalytic activity for the reduction of nitroaromatic compounds.

The reduction of nitroaromatic compounds are highly required reactions as the amino groups are essential in many pharmaceutically important compounds, in agro industry, large compounds of dyes. The easy and greener way is to use the metal nanoparticles which show excellent catalytic properties. In the literature, a few procedures involving noble metal NPs such as Pd, Pt, Ag, Au, as well as Fe, Fe_3O_4@Ni and Ni@Ag NPs have been demonstrated for the reduction of nitro groups.[6,7,8] But these conventional methods have large limitations like requirement of high H_2 pressure, organic solvents, high temperature, complicated operational procedure, prolonged reaction time, poor selectivity and many side products. In the work, efforts have been carried out using bimetallic nanoparticle doped rGO as the potential catalyst with an easy procedure of synthesis and tremendous catalytic activity in the reduction of nitroaromatic compounds.[9, 10]

1.2. Graphene

Graphene is a single layer of sp^2-hybridized carbon atoms arranged in a two-dimensional lattice; it has attracted much attention in the past few years for its exceptional thermal, mechanical, and electrical properties. One of the most promising applications of this material is in the synthesis of nanocomposites, where it acts as a support system for nanoparticles. It is regarded as the "thinnest material in the universe" with tremendous application potential. Graphene is predicted to have remarkable properties such as high thermal conductivity, superior mechanical properties and excellent electronic transport properties .[11]

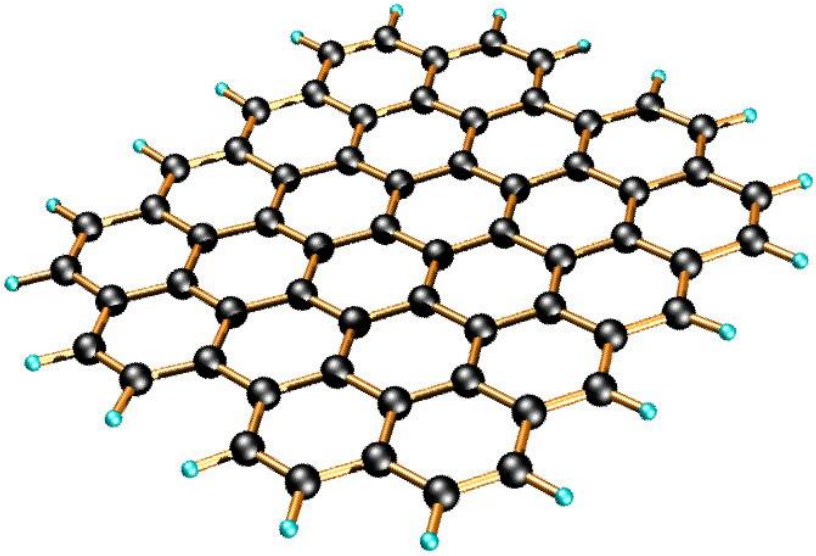

Fig.1. A layer of graphene. [12]

1.3. Graphene Oxide: Structure

GO has emerged as a precursor offering the potential of cost-effective, large-scale production of graphene-based materials. Graphene oxide is considered as a precursor for graphene synthesis. GO is usually prepared by oxidation of graphene followed by dispersion of graphene in any polar or non-polar solvent. Various models picture it as a graphene layer with various oxygen containing functional group like hydroxyl, ether, carboxylic, keto groups.

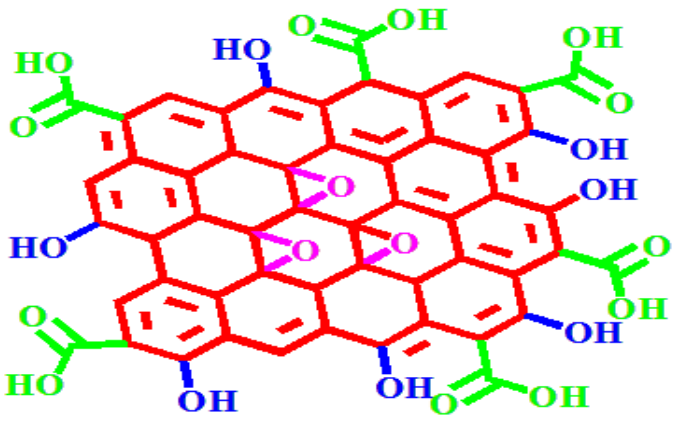

Fig.2. A layer of graphene oxide.[13]

1.4. Graphene Oxide: Properties and Application

GO has various in homogeneities depending on its method of preparation. In fact, the ideal stoichiometry has never been achieved. The presence of these groups has functionalized and enhanced the property of graphene oxide but on the other hand it has decreased its electrical conductivity. By appropriate tuning of these functionalized groups the properties of graphene oxide can be changed as requirement. [14]

Graphene oxide is normally synthesized by hummer's method. In this method graphite and sodium nitrate in sulphuric acid was heated at 66 °C which is then cooled to 0 °C. Potassium permanganate is then added to the solution and stirred. Various modifications of these method have been developed for enhanced production of graphene oxide.[15]

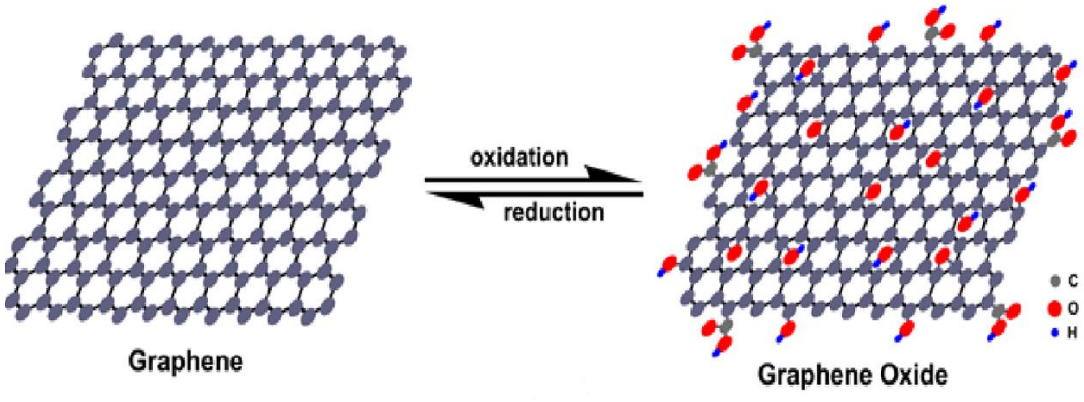

Fig.3. Oxidation of graphene to graphene oxide and reduction of graphene oxide to graphene.

One of the major advantages of graphene oxide is that it can act as a support for nanoparticles to synthesize catalyst. The other applications are to provide a tunable platform for optical applications. Defunctionalising it leads to formation of graphene which has its own other applications. GO can be used as precursors to bulk scale production of an assortment of exfoliated CMGs or 'graphite nanoplatelets' for use as a filler. [14, 16]

1.5. Reduced Graphene Oxide

Removal of oxygen moieties from the graphene oxide layers lead to the formation of reduced graphene oxide. Reduction of graphene oxide tunes its properties and can lead to excellent catalytic activity which exclusively depends on the number of oxygen moieties. Parameters affecting the oxygen functionalization such as heat, moisture, defects or intercalants in reduced GO (rGO), tailor the materials optical, electrical, mechanical, and physical properties.

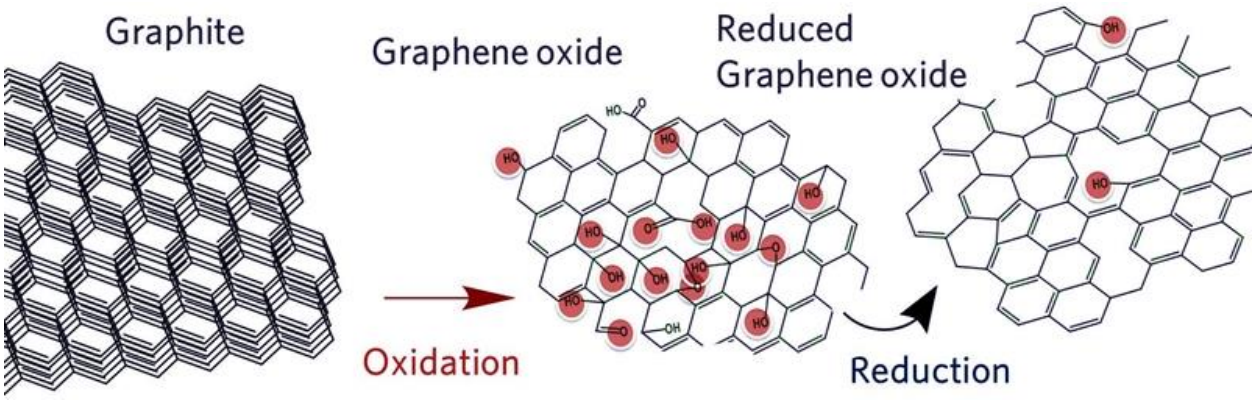

Fig.4. Oxidation of graphene to graphene oxide and reduction of graphene oxide to reduced graphene oxide.

1.6.Nanocomposites

Nanocomposites are materials that incorporate nanosize particles into a matrix of standard material. The result of the addition of nanoparticles is a drastic improvement in properties that can include mechanical strength, toughness and electrical or thermal conductivity. The effectiveness of the nanoparticles is such that the amount of material added is normally only between 0.5 and 5% by weight. They have properties that are superior to conventional micro scale composites and can be synthesized using simple and inexpensive techniques. Materials are needed to meet a wide range of energy efficient applications with light weight, high mechanical strength, unique color, electrical properties and high reliability in extreme environments. Applications could be as diverse as biological implant materials, electronic packages, and automotive or aircraft components. Although some of the properties will be common between the applications, others will be quite different. An electronic package polymer composite must be electrically insulating, while an aircraft component may need to be electrically conductive to dissipate charge from lightning strikes.[17]

1.7.Reduced-Graphene Oxide Based Nanocomposites

Reduced-Graphene oxide with a varying structure is widely used as a support system. Due its functionality it can be easily dispersed in any solvent and has tunable properties. The crinkly structure of rGO can support aggregation of a lot of nanoparticles. These nanocomposites have a very high surface area and high density which provide excellent catalytic activity. Also, due to

the strong interaction between the metallic nanoparticles and rGO, many properties are enhanced and they are easily synthesized without any surfactant. [18, 19]

1.8. Synthesis of Reduced-Graphene Oxide Based Nanocomposites

The synthesis of metal nanoparticles doped on graphene oxide usually uses co reduction method. The graphene oxide and the metal precursors are simultaneously reduced by a strong reducing agent under constant stirring. Due to the vigorous stirring, the metal starts doping on the rGO surface. [20-22]

1.9. Approaches for Preparing Nanoparticles

There are two approaches for preparing nanoparticles: Top-Down and Bottom-Up. Top-Down approach deals with breaking down of bulk materials into nano dimensional particles. Bottom-Up approach deals with constituting of nanoparticles from individual atoms.

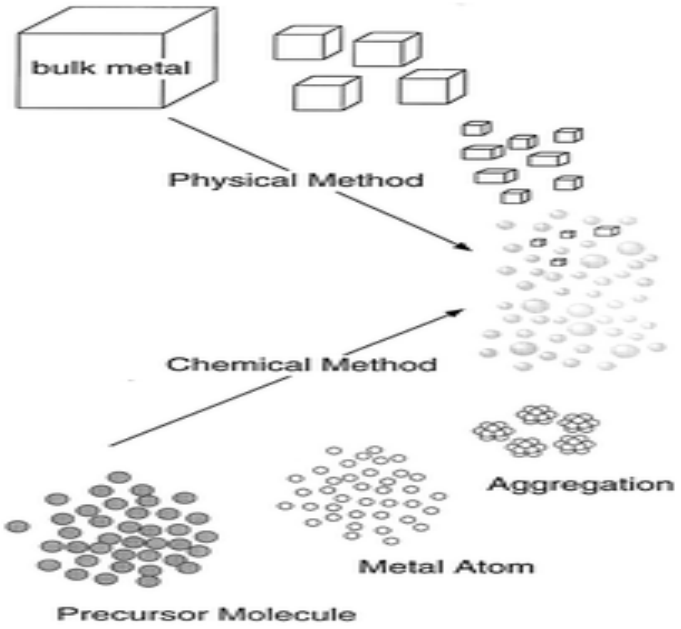

Fig.5. Top-Down and Bottom-Up Approach of nanomaterials synthesis.[23]

1.10. Bimetallic Nanoparticles

The bimetallic nanoparticles are more stable and effective than the individual constituent monometallic nanoparticles. This has made the design and synthesis of bimetallic nanoparticles considerably popular. The bimetallic nanoparticle exhibit characteristics of both the constituent metals and have an enhanced catalytic capacity. Bimetallic catalytic systems can potentially achieve chemical transformations that are unprecedented with monometallic catalysts because different components of the catalyst have a particular function in the overall reaction mechanism.

Since bimetallic nanocrystals are composed of two different metal atoms, the atomic distribution can greatly influence the final architectures of nanocrystals, which could have a significant impact on their catalytic performance. Although, significant progress has been made in the controllable synthesis of nanocrystals with well-defined composition, structure, size, and morphology in recent years, more accurate control over nucleation and growth stages is required to achieve formation of bimetallic nanocrystals. Bimetallic nanomaterials can emerge with various architectures including, core—shell structure and alloyed structure. Different synthetic strategies have been developed to prepare bimetallic nanocrystals with well-defined architectures.[24]

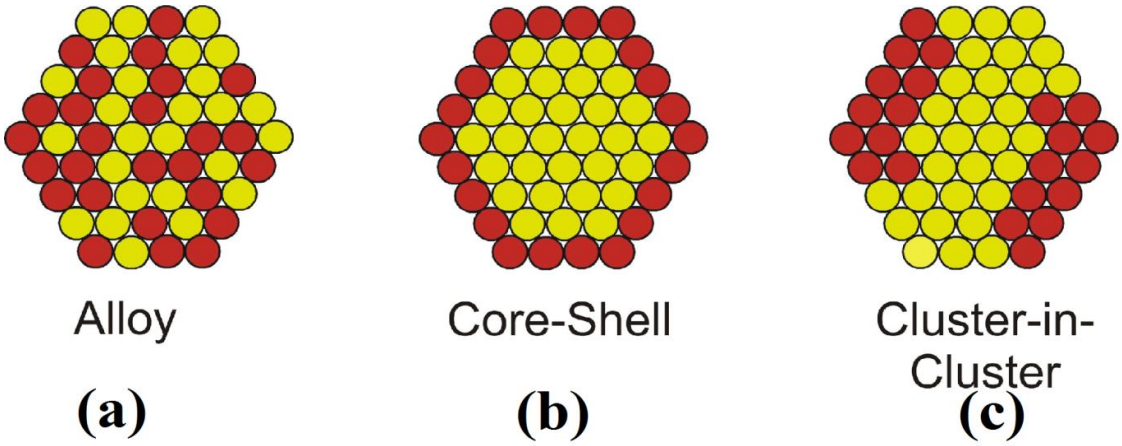

Fig.6. Types of bimetallic nanoparticles: a) Alloy nanoparticle b) core-shell nanoparticle c) Cluster in cluster nanoparticle.

1.11. Methods of Synthesis of Bimetallic Nanoparticles

The basic type of method of synthesis of bimetallic nanoparticles are:1)Co-reduction method and 2) Sequential reduction method.

1.11.1. Co-reduction Method

Co-reduction method is the simplest method for synthesis of bimetallic nanoparticles. The metal precursors are simultaneously reduced by a strong reducing agent to produce alloy nanoparticles. It is similar to the monometallic nanoparticle synthesis but differs only in the number of metal precursors.

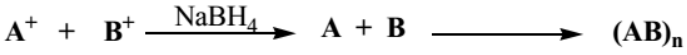

Scheme.1. Schematic Representation of Co-reduction method.

In above schematics it can be found that the two metal precursors A and B are added in the same solution then a strong reducing agent is added to reduce them simultaneously into bimetallic alloy nanoparticles.

1.11.2. Sequential Reduction Method

This method is used for the synthesis of core-shell particles. Usually the two metals used for making the nanoparticles have different reducing capacity for different solvents. So one of them is first reduced then the second metal forms a layer over the first one ,i.e., they are added in the system one after another with reducing agent already present in the system.[11]

Scheme.2. Schematic Representation of the Sequential reduction method

As shown in the above scheme the metal precursor A is first reduced with a strong reducing agent, then a mild reducing agent reduces the second metal precursor over the first formed A metal nanoparticle to give a core-shell bimetallic nanoparticle.

1.12. General Characterization Techniques Used for Nanoparticles

The general characterization techniques generally used for the synthesized materials are as described below:

Techniques	**Characteristics Identified**
Transmission electron microscopy(TEM)	Core Size, Morphology, Atomic coordinates
Energy Dispersive X-Ray Spectroscopy (EDXS)	Elemental Distribution
X-Ray Diffraction(XRD)	Crystal structure, Particle size
X-Ray photoelectron spectroscopy (XPS)	Oxidation state, Electronic Interaction
Scanning Electron Microscope(SEM)	Topological information of the sample
Field Emission Scanning Electron Microscopy(FESEM)	Atom size and other topological information of the sample
Ultraviolet(UV)-Visible spectroscopy	Plasmon bands, presence of aggregates
Infrared (IR) Spectroscopy	Surface structure

1.13. Reduction of Nitro Group

The reduction of nitro group to amino group is a vital process for pharmaceutical, agro, polymers and dyes industry. One example can be taken as the reduction of p-nitrophenol to p-amino phenol which is an analgesic. Also, in dyes industries, the reduction of nitro group in very complicated molecules is required in higher amount with good selectivity. A catalyst with a poor selectivity is not appropriate. For large scale production of amine group we need a fast catalyst which can catalyze this reaction. [10, 25-27] The process should be green in all aspects without the use of large amount of organic solvents. The selective reduction of nitro group requires stoichiometric amount of reducing agent. Many processes have been cited in literature for this reaction but there is a production of side products like hydroxylamine and hydrazine.[9] The main limitations of earlier reported work were the necessity of high H_2 pressures, prolonged reaction times, lower turnover numbers, organic solvents and high temperatures. Due to these limitations, the good productivity and selectivity were not found. Also, the process becomes cumbersome

and unsafe to be handled. A huge amount of H_2 requirement and high temperature makes the process accident prone.

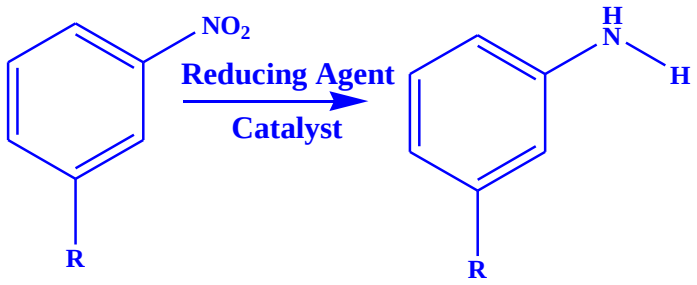

Scheme.3. A general scheme for reduction of nitroarene to aminoarene.

Further, the selection of metal and its support, the hydrogen source and operational simplicity, which are the important parameters for effective conversions, are restricted. Also when these processes are metal catalyzed, they are required in large amounts and so the conventional methods are not cost effective. However, an alternative procedure which is efficient, simple, chemo selective, green and cost-effective would be highly beneficial. A process with higher efficiency and good selectivity can make it industrial. [28, 29]

1.14. Objective

The high catalytic activity of Au and Cu nanoparticles has been reported in literature. [30-32] Also the catalysis process carried on graphene oxide is also reported. The objective of this work is to produce alloy bimetallic Au-Cu nanoparticles supported on graphene oxide layers to combine their properties and observe their catalytic activity to reduce various nitroarene to amino arenes at room temperature with the help of reducing agent like sodium borohydride. The main objectives are enlisted as follows:

- To synthesize monometallic and bimetallic Au-Cu nanoparticles supported on reduced graphene oxide using co-reduction method.
- To characterize the synthesized catalysts using different characterization techniques such as UV-Vis, XRD, TEM/SAED, FESEM, and EDX.
- To observe it's catalytic activity for reduction of various nitroaromatic compounds such as p-nitroaniline, p-nitro phenol, o-nitrobenzoic acid, p-nitro benzoic acid and m-nitrobenzoic acid.

- To compare its catalytic activity with different catalysts i.e. Au/rGO nanocomposites and Cu/rGO nanocomposites.
- To investigate the catalytic activity by varying the concentration of the reducing agent like sodium borohydride.
- To evaluate the catalytic activity by varying the amount of the catalyst.

1.15. Importance of Our Work

In the present work we tried to synthesis graphene oxide supported gold-copper bimetallic nanoparticles. Gold has been investigated as very good reducing catalyst in organic reactions. The catalytic activity varies with the size of the nanoparticles. At extremely small size, the quantum effect predominates and the surface atoms are very high in number which is the prime reason for high catalytic activity. It works at considerably low temperatures but requires nitrogen atmosphere and a suitable surfactant for its stability. [30, 32] Similarly copper, has a high reducing capacity but again it is oxidized in air and not easily handled. Still it is extensively used for the formation of carbon-carbon and carbon-heteroatom bonds. [31] So, these two metals were allowed to form bimetallic nanoparticles to incorporate beneficial properties of both the metals. They are supported on graphene oxide layers to provide large surface area and stability.

Chapter 2

EXPERIMENTAL

2.1. Materials

Copper nitrate trihydrate extrapure (M.W-241.60 g/mol) and 99.9% pure Chloroauric Acid trihydrate (M.W.-393.83 g/mol) were bought from Himedia and Sigma Aldrich respectively. Sodium Borohydride granules with 10-40 mesh (M.W.-37.83 g/mol), p-nitrophenol (M.W.-139.11 g/mol), o-nitrobenzoic acid (M.W.-167.12 g/mol), p-nitrobenzoic acid (M.W.-167.12 g/mol), m-nitrobenzoic acid (M.W.-167.12 g/mol), p-nitroaniline (M.W.-138.12 g/mol)were bought from Sigma Aldrich. Graphite powder, $CDCl_3$ and $SnCl_4.5H_2O$ were purchased from Sigma-Aldrich. H_2O_2 (30%), isopropanol, ethanol, $NaNO_3$, H_2SO_4 (98%), HCl, $KMnO_4$, and silica gel (100–200 mesh) were purchased from Hi-Media. All chemicals were used as received without further purification. 18 MU cm Milli-Q water was used throughout the synthesis.

2.2. Synthesis

2.2.1. Synthesis of graphene oxide (GO)

GO was prepared from natural graphite powder through modified Hummer's method. [33-35] In a typical synthesis, 1 g of graphite was added to 25 ml to conc. H_2SO_4 (98% w/w), followed by stirring at room temperature for 24 h. After that 100 mg of $NaNO_3$ was added to the mixture and stirred for 30 min. Subsequently, the mixture was kept below 5 °C using an ice bath, and 3 g of $KMnO_4$ was slowly added to the mixture and the mixture was stirred for 2 h under ice-water bath. About 250 ml distilled water and 20 ml H_2O_2 (30%) was added to dilute the solution at room temperature. The suspending solution was allowed to precipitate for 12 h and later on, the upper supernatant was collected and centrifuged. Successively, the GO powders were washed with 10% HCl and distilled water three times. The obtained GO was dispersed in distilled water to get a stable brown solution.

2.2.2. Synthesis of Cu doped Graphene Oxide:

100 mg of graphene oxide was added to 80 ml of water in a round bottom flask and sonicated for 1 hour. To the mixture 10 ml of 0.056 mmol Cu $(NO_3)_2$ was added and it was heated at 180 °C for 1 hour under constant stirring and N_2 atmosphere. Meanwhile a solution of 0.56 mmol $NaBH_4$ in 10 ml was made and added to the reaction mixture dropwise.

2.2.3. Synthesis of Au doped Graphene Oxide

100 mg of graphene oxide was added to 80 ml of water in a round bottom flask and sonicated for 1 hour. 10 ml of 0.056 mmol of $HAuCl_4$ was added to the mixture and it was heated at 180 °C for 1 hour under constant stirring and N_2 atmosphere. In the meantime a solution of 0.56 mmol $NaBH_4$ in 10 ml was made and added dropwise under vigorous stirring.[36]

2.2.4. Synthesis of Au-Cu/r-Graphene oxide

100 mg of graphene oxide was added to 80 ml of water in a round bottom flask and sonicated for 1 hour. To the mixture 0.028 mmol Cu $(NO_3)_2$ and 0.0280mmol of $HAuCl_4$ was added and it was heated at 180 °C for 1 hour under constant stirring and N_2 atmosphere. Meanwhile a solution of 0.56 mol of $NaBH_4$ in 10 ml was made and added to the mixture drop wise. Then the mixture was quickly heated to 180 °C for an hour and it was cooled to 120°C.Then it was vigorously stirred and was heated to 160 °C under N_2 atmosphere .[36, 37]

2.3. Reduction of Nitroaromatic compounds

The catalytic reduction of p-nitro aniline and other nitroaromatic compounds were studied. To study the effect of the dosage of catalyst, the amount of catalyst was varied in the range of 0.5-3.0 mg/ml. The initial concentration of p-nitro aniline was taken as 0.01 M and the concentration of $NaBH_4$ was 0.05 M. 2 ml of nitroaniline compound was added to 1 ml of 0.05 M $NaBH_4$. After adding catalyst, the p- nitro aniline was converted to p-phenyl diamine. The initial absorbance was taken using the UV-Vis spectrometer. The effect of concentration of $NaBH_4$ was studied between the range of 0.03 M-0.07 M, keeping the initial concentration of nitro aromatic compound as 0.01 M and catalyst dose of 2 mg.

2.4. Characterizations

The nanoparticles synthesized in the above sections were characterized by UV-Visible spectroscopy (UV-Vis), X-Ray diffraction (XRD), Scanning Electron Microscopy (SEM), Field Emission Scanning Electron Microscopy (FESEM) and Transmission Electron Microscopy (TEM):

UV-Vis Spectroscopy

UV-Vis Spectra of the catalysts were recorded by Shimadzu spectrophotometer (UV-2450) in the range of 200-900 nm. The catalytic activity of the prepared catalysts was also measured using UV-Vis spectroscopy.

X-ray Diffraction

The X-ray diffraction patterns of the Au-Cu/graphene oxide, Au doped graphene oxide, Cu doped graphene oxide and Au-Cu bimetallic nanoparticles were recorded on a Phillips PAN analytical diffractometer using Ni-filtered $CuK_{\alpha 1}$ radiation. The XRD measurements were carried out 20-80 degree for both the samples, respectively with a scan speed of 5 degrees per minute.

Scanning Electron Microscopy

Scanning electron microscopy was taken using JEOL JSM-6480 LV microscope (acceleration voltage 15 kV). The sample powders were deposited on a carbon tape before mounting on a sample holder for SEM analysis. EDX analysis shows the presence of Au-Cu nanoparticles on graphene oxide framework.

Field Emission Scanning Electron Microscopy

Field emission SEM was taken by Nova Nano SEM/FI microscope with ultra-stable, high current Schottky gun having a beam landing energy down to 50 V and resolution: 1.4 nm @ 1 kV without beam deceleration for all the catalysts.

Transmission Electron Microscopy

TEM measurement was taken to confirm the presence of bimetallic nanoparticle (Au-Cu) on the surface of reduced graphene oxide. TEM was taken using Philips, Holland CM-12.

Chapter 3

Results and Discussion

Au, Cu and Au-Cu bimetallic nanoparticles doped reduced graphene (rGO) were synthesized by direct reaction between graphene oxide and the metal precursor, and simultaneously reduced using sodium borohydride. In order to investigate the transformation of graphene after doping Au-Cu bimetallic NPs the samples were characterized using various techniques which are explained below.

3.1. UV-Vis Study

UV-Vis study is an important technique to characterize the structural changes of graphene after doping. Fig.7. depicts the UV-Vis spectra of graphene oxide, monometallic Au, Cu doped rGO and bimetallic Au-Cu doped rGO. For GO, two characteristic absorption peaks are observed in UV-Vis spectra, a maximum at 230 nm which can be attributed due to $\pi \rightarrow \pi*$ transition of aromatic C-C bond and a shoulder at 303 nm, from $n \rightarrow \pi*$ transition of C=O bond.[38]

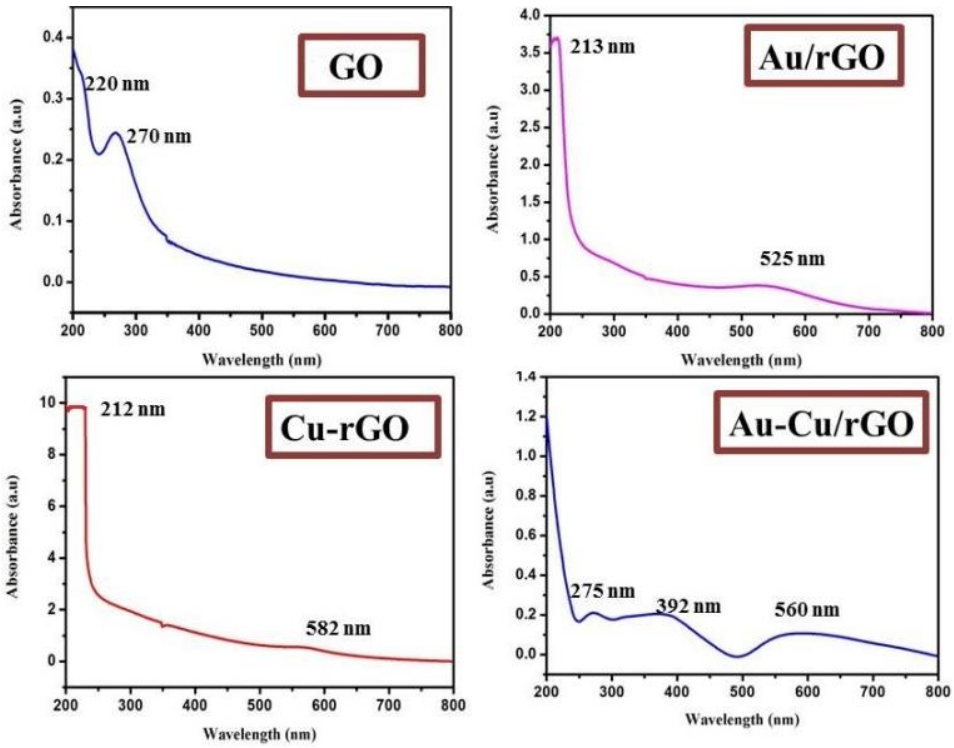

Fig.7. UV-Vis spectra of synthesiszed catalysts.

The original electronic conjugation is restored during reduction of GO to rGO by sodium borohydride and a characteristic absorption peak of rGO has been observed at around 270 nm, whereas the shoulder at 303 nm disappears. The incorporation of monometallic and bimetallic Au, Cu nanoparticles can be confirmed as follows. The Au/rGO presents a single and strong absorption peak at around 525 nm is due to the surface plasmon resonance of gold nanoparticles, while Cu-rGO shows an absorption peak at around 582 nm. For Au-Cu/ rGO, the surface plasmon band can be observed in between Au/ rGO and Cu/ rGO. The maximum absorption peak of rGO suspension is at 270 after doping the peak red shifted this shows that the rGO was also reduced and the electronic conjugation within the graphene nanosheets are restored during the doping process.

3.2. XRD Study

X-ray diffraction pattern of GO, Au/rGO, Cu/ rGO and Au-Cu/ rGO are presented in Fig. 8. The XRD pattern of GO shows a sharp peak at around 2Θ= 10.5 corresponds to (001) of GO. [39] Further the XRD pattern of GO gives broad peak at 2Θ= 25.05 which corresponds to (002) reflection of reduced graphene oxide. The broad peak demonstrates that there is decrease in crystallinity on reducing graphene oxide to reduced graphene oxide.

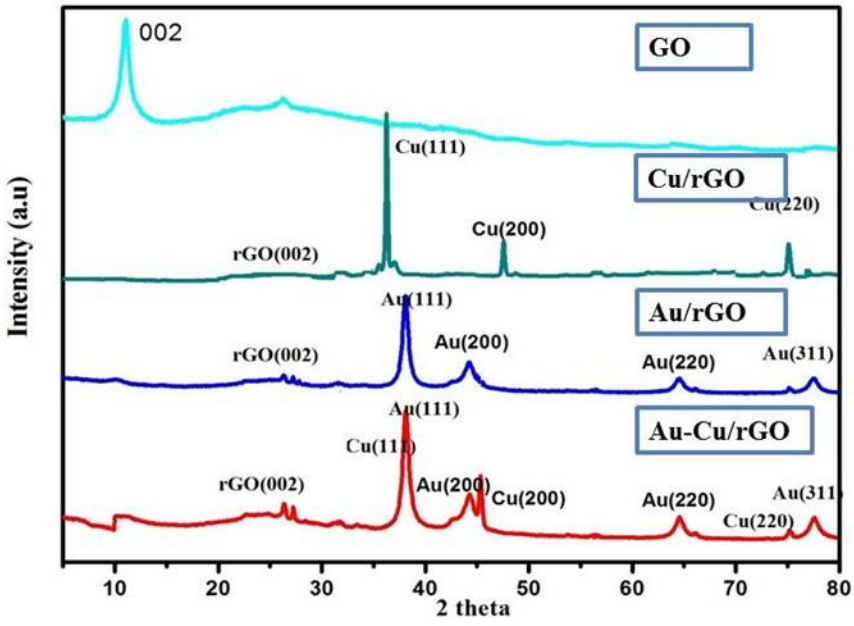

***Fig.8. XRD pattern of different catalysts*.**

On the other hand, Au/rGO shows a diffraction peak at 2Ɵ= 38.3, 44.1, 64.11 and 74.5 which can be indexed as (111), (200), (220) and (311) (JCPDS card no. 02-1094) due to Au nanoparticles Similarly, Cu/rGO presents the diffraction peak at 2Ɵ=36.06, 47.54 and 73.9 which can be further indexed as (111),(200), and (220), which is due to the presence of metallic Cu nanoparticles as well as a broad peak due to rGO. The diffraction peaks of bimetallic Au-Cu/rGO are positioned in between Au/rGO and Cu/rGO. The diffraction peaks of Au-Cu/rGO are positioned at 2Ɵ=38.17, 44.14, 45.8, 64.3, 75.2 and 77.7, which corresponds to Cu (111), Au(111), Au (200), Cu (200), Au (220), Cu (220), Au (311). The presence of low intensity broad spectra at 2Ɵ is due to the presence of rGO. The peaks are due to metal nanocrystals are broad, indicating nanocrystalline size and strain due to incorporation within graphene nanosheets. The position of (002) peak of graphene does not change for different metal hybrids.[39] Moreover, as compared to Au/rGO, and Cu/rGO the Au–Cu/rGO sample shows broader XRD peaks, suggesting that the Au–Cu alloy has a smaller particle size than the monometallic counterparts.

The particle size of bimetallic Au-Cu NPs was estimated by Scherrer's equation:

$$D=K\lambda/B\ Cos\theta$$

Where, D is the average diameter in nm, K is the Scherrer constant (0.89), λ is the X-ray wavelength (λ=0.15418 nm), B is the corresponding full width at half maximum (FWHM) of the diffraction peak, and Ɵ is the Bragg diffraction angle. The particle size was calculated from (111) crystal plane and the particle size was found around 7 nm for bimetallic Au-Cu NPs which is very close to the TEM result as discussed later. The broadness of the peak is the indication of the presence of graphene nanosheets with varying d-spacing values.

3.3. FESEM Study

The detailed structural and morphological characterization of GO and Au-Cu/rGO was carried out using FESEM. Fig. 9.shows the FESEM image of reduced graphene oxide which reveals the crumbled and scrolled morphology of graphene sheets. The layers of graphene sheets are clearly visible in Fig. 9.

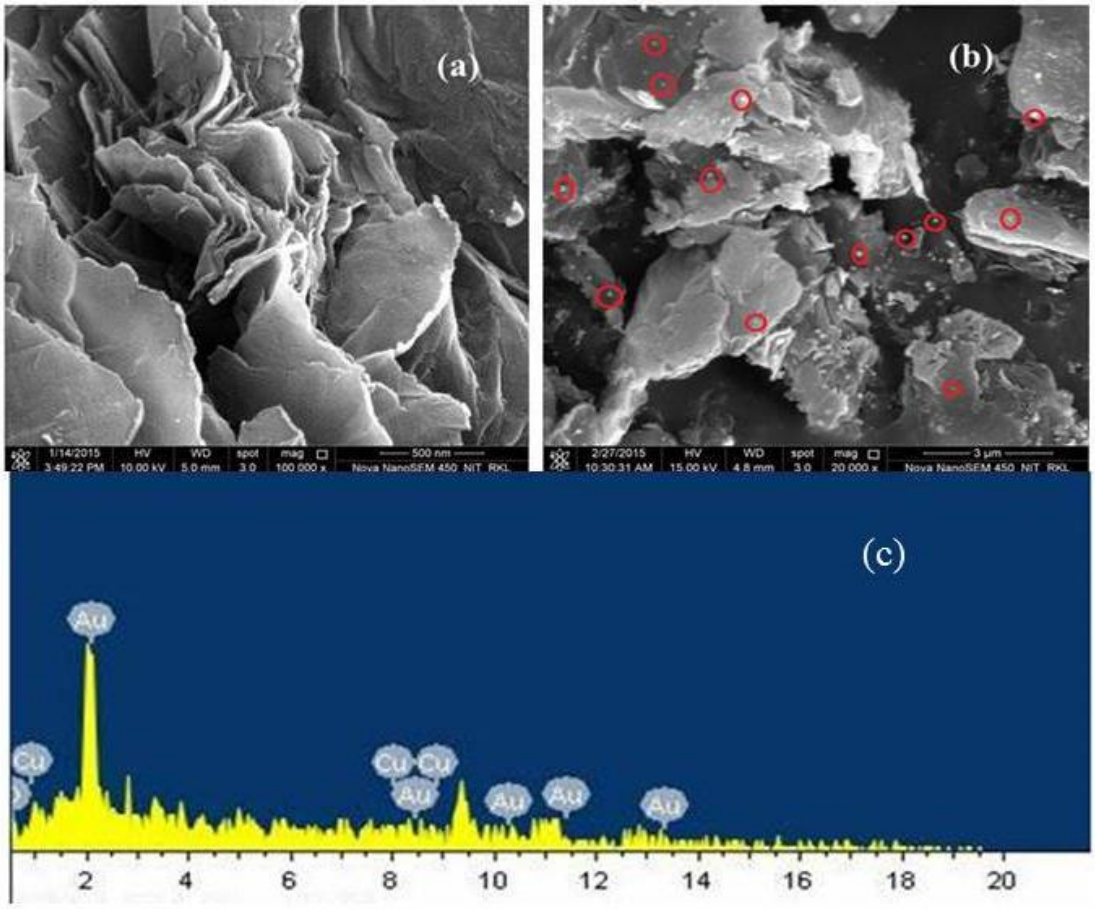

Fig. 9. FESEM image of (a) rGO, (b) Au-Cu bimetallic nanoparticle doped reduced GO and (c) EDX spectra of Au-Cu/rGO

At the other hand FESEM image of Au-Cu/rGO is shown in Fig. 9, shows the presence of small nanoparticle on the surface of graphene sheet. The nanoparticles were homogeneously distributed on the surface of reduced graphene oxide**.** EDX spectra show the presence both the metal nanoparticle on reduced graphene oxide frees from other impurities.

3.4. TEM/SAED Study

The detailed morphology and structure of graphene and Au-Cu nanoparticles doped reduced grapheme oxide have been characterized thoroughly by TEM imaging. It is to be noted that TEM samples were prepared by dropping the sonicated dispersion of sample in ultrapure methanol

onto 600 mesh copper grids coated with lacy carbon and dried at room temperature for 3 hours. Fig. 10 displays TEM images of as-prepared Au-Cu/rGO nanocomposites.

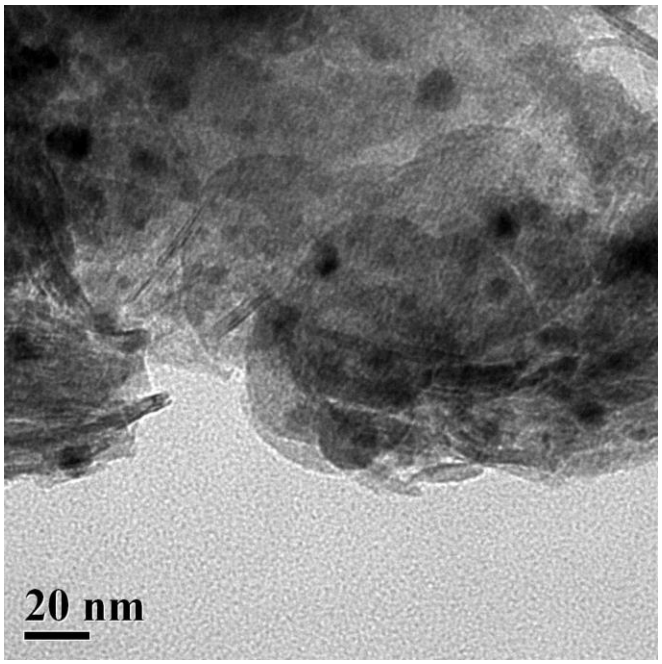

Fig. 10. TEM image of Au-Cu/rGO catalyst.

Fig. 10 (a). reveals that the nanoparticle are uniformly distributed on the rGO surface, and a continuous sonication for 2 min before TEM characterization does not remove any NPs from the graphene surface (no NPs were present on the TEM carbon film), which confirms a strong interaction between NPs and rGO. The average diameters of the bimetallic Au-Cu nanoparticles were found to be 6.5± 0.5 nm.

3.5. Catalytic Activity

3.5.1. Catalytic Reduction of *p*-Nitroaniline and Other Nitro Aromatic Compounds

3.5.1.1. Catalytic Activity of Monometallic and Bimetallic NPs doped rGO

As synthesized monometallic Au, Cu and Au-Cu/G has been used as a catalyst for reduction of nitroaromatic compounds using sodium borohydride as reducing agent and water as a solvent as shown in scheme 4.

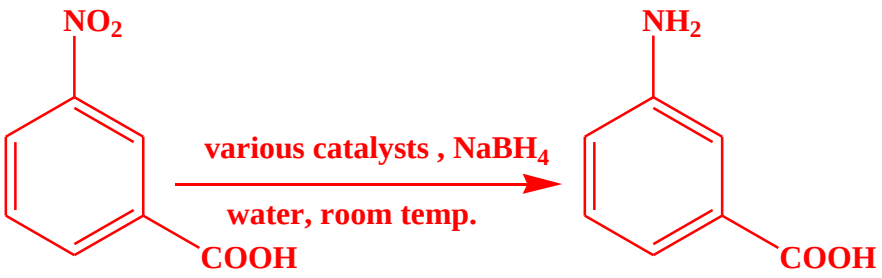

Scheme.4. Model reaction for reduction of MNBA to MABA using various catalysts.

Initially, reduction of m-nitrobenzoic acid (MNBA) was investigated using monometallic reduced graphene oxide (rGO), Au, Cu and bimetallic Au-Cu in rGO as catalyst. Among all, Au-Cu/rGO was found to be the most efficient catalyst for the reduction of m-nitrobenzoic acid. The initial reduction process of p-nitroaniline to p-phenyldiamine was demonstrated under various conditions. The conversion was monitored using UV-Vis spectroscopy where the reactant and product displays different absorption peaks at 286 nm and 241 nm, respectively as shown in Fig 12. The changes in the UV–vis absorption spectrum of MNBA during the reaction time are shown in Fig. 12. The peak intensity of MNBA at about 286 nm rapidly decreased and the peak disappeared in 10 min.

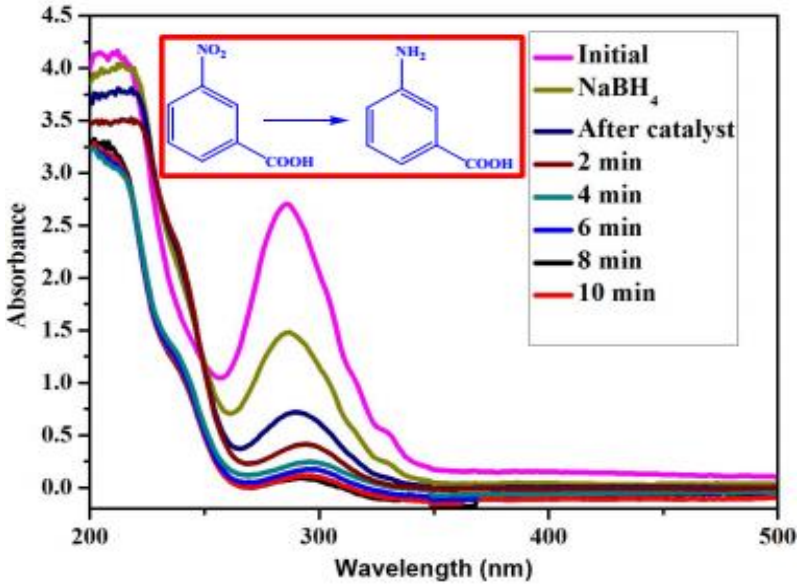

Fig.11. Absorption spectra of MNBA to MABA using Au-Cu/rGO catalyst

This depicts that the reduction of MNBA was complete in 10 min. For comparison, the reactions of MNBA, with Au/rGO and Cu/rGO were also investigated under the same condition as shown in Fig. 13. which depicts that as compared to Au/rGO and Cu/rGO, Au-Cu/rGO, shows better catalytic activity for reduction of MNBA.

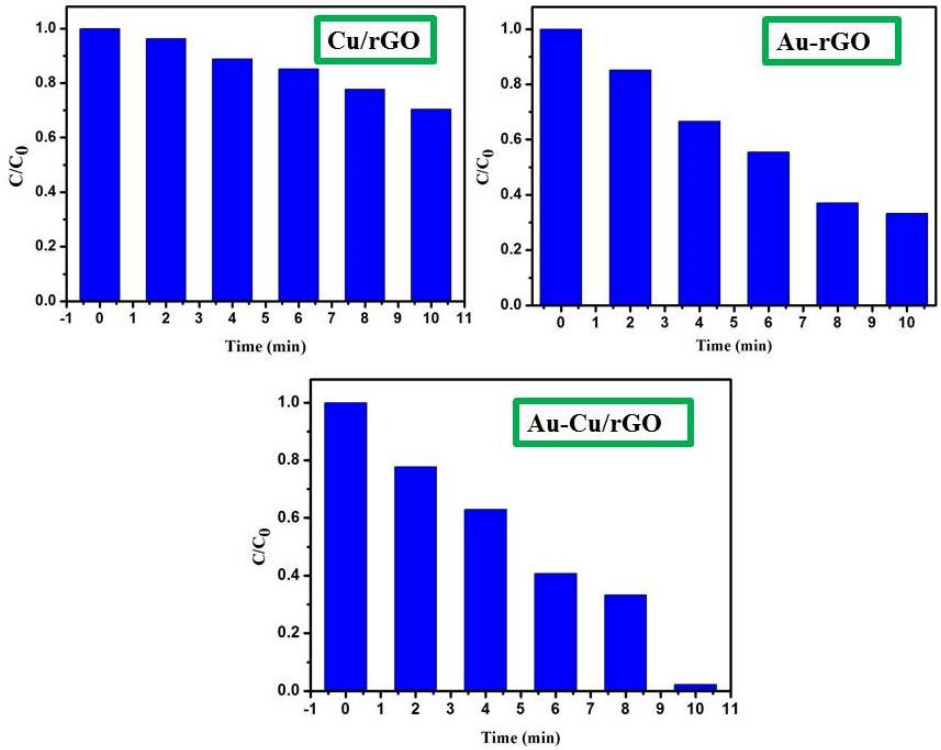

Fig.12. Plots for reduction of MNBA using Cu-rGO, Au-rGO and Au-Cu/rGO

3.5.1.2. Effect of Catalyst Dose

The influence of catalyst was studied by keeping the concentration of $NaBH_4$ as 0.05 M. The model reaction of reduction p-nitroaniline (PNA) to p-phenyl diamine (PPDA) scheme 5. was taken in consideration to study the effect of various catalyst doses in the reaction.

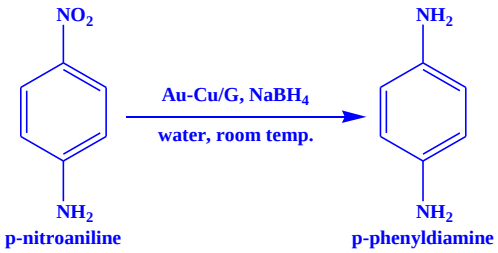

Scheme 5. Model reaction involving reduction of PNA to PPDA

The effect of the dosage of catalyst was investigated varying the amount from 0.5 mg to 3 mg. The rates of the catalytic reduction of nitroaniline compounds increased by increasing catalyst dosage. The rates of the catalytic reduction were constant after dosage of 2 mg on further increasing the catalyst dose very minimal change was found as shown in Fig. 14. Therefore, 2 mg of catalyst was taken as optimum catalyst dose and was used in further experimental study.

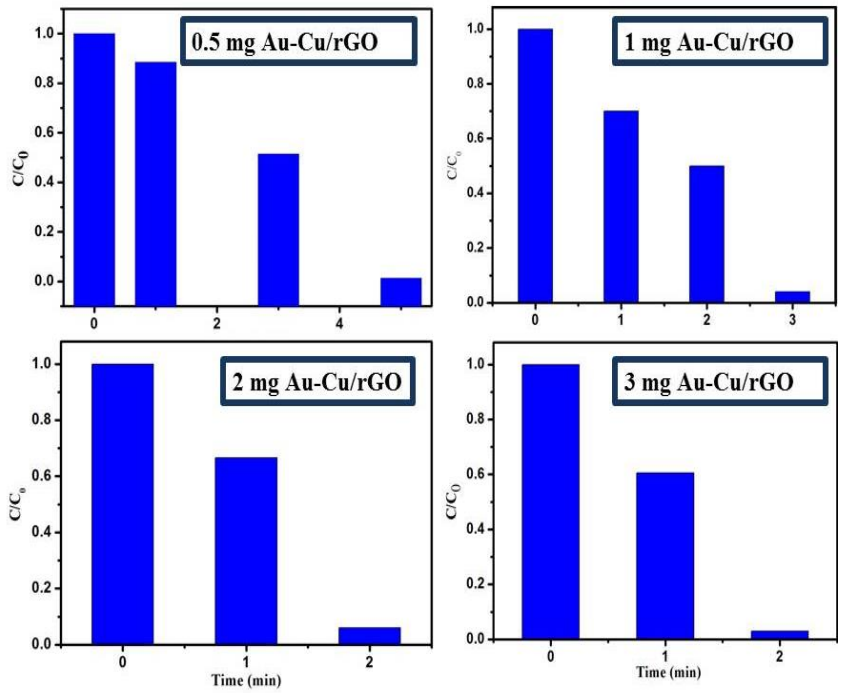

Fig.13. Reduction of PNA to PPDA with change in catalyst dose.

3.5.1.3. Effect of $NaBH_4$ Concentration

The influence of $NaBH_4$ concentration was also studied by considering the model reaction as given earlier in scheme 2.

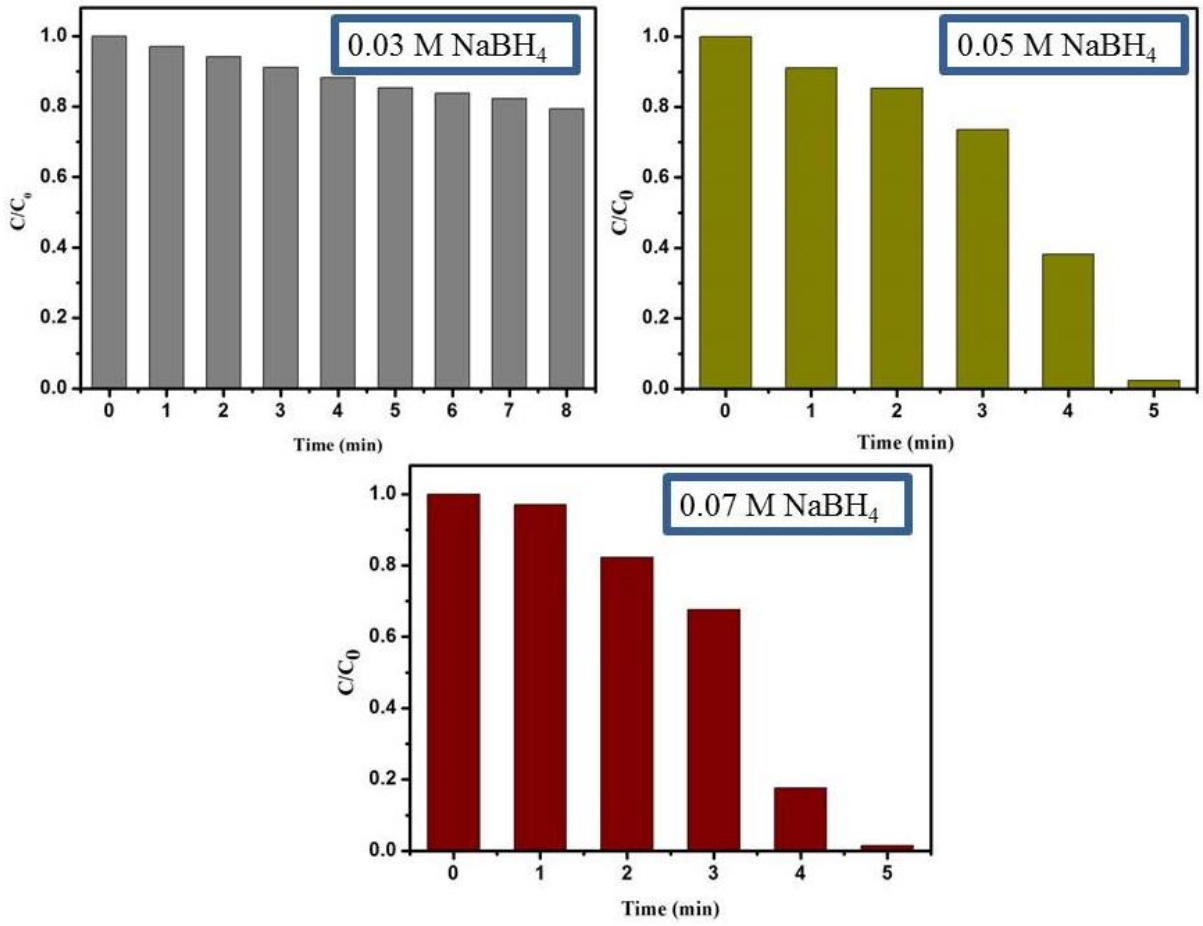

Fig.14. Reduction of PNA to PPDA with change in $NaBH_4$ concentration

The effect of the concentration of $NaBH_4$ on the catalytic reduction was also investigated keeping the catalyst amount of 2 mg. The rates of the catalytic reaction of nitroaniline compounds significantly increased until $NaBH_4$ concentration was 0.05 M. After this concentration, the rates of the catalytic reaction were constant. Therefore, we used 0.05 M $NaBH_4$ in all experiments. Fig.15. shows the reduction rate of nitroaniline compound using various concentration of sodium borohydride. As it can be observed from the Fig. 15. that on taking 0.03 M of reducing agent no reduction is happening

.

.

3.5.2. Mechanism

In this study, a six electron transfer process takes places between nitroaniline compounds and the reducing agent $NaBH_4$. Basically in this heterogeneous catalysis, reaction occurs in four different steps as follows: Firstly, the adsorption of the nitroaniline compounds to the nanocatalysts, secondly, diffusion of the nitroaniline compounds on the active site, thirdly, reaction of the nitroaniline compounds to form the adsorbed product, and finally, desorption of the nitroaniline compounds from the surface. The slowest step determines the rate of the reaction. [40] In this present study, the sequential electron transfer between nitro compound and $NaBH_4$ plays the major role on the critical rate-limiting step under the current experimental conditions. Saha et al. observed that the reduction of 4-NA was catalyzed by calcium alginate-stabilized Ag and Au nanoparticles via zero-order kinetic model.[41]

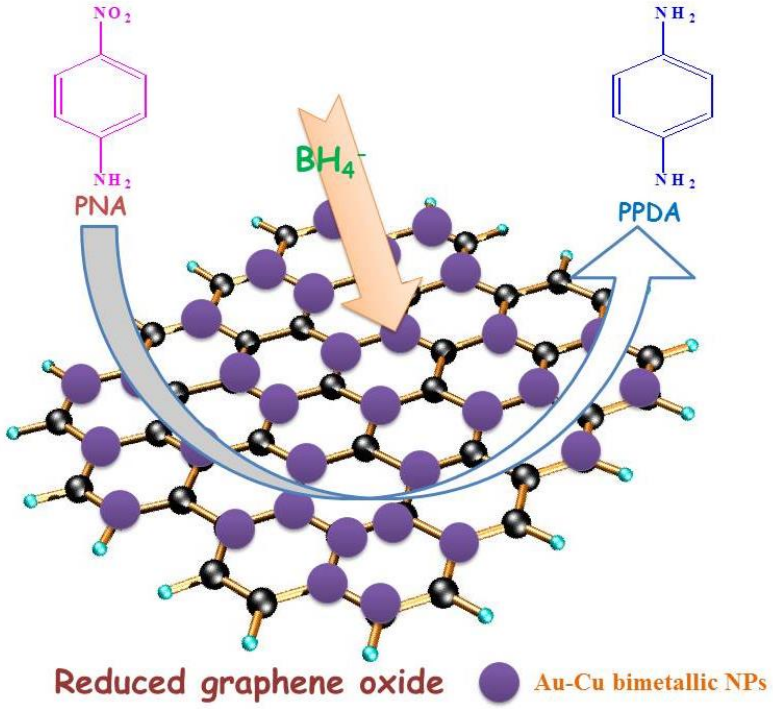

Fig. 15. Schematic representation of reduction of p-nitroamine to p-phenyldiamine

Fig.16. shows the schematic mechanism of reduction of p-nitroaniline to p-phenyl diamine.

3.6.3. Reduction of Other Nitroaromatic Compounds

While the absorbance value of PNA decreases, the absorbance value of PPDM increases in the catalytic reduction process as discussed previously. To ensure if such an enhancement toward reduction of nitro organics is general, we had further investigated the photo catalytic performance of Au-Cu/rGO towards selective reduction of nitro aromatic groups

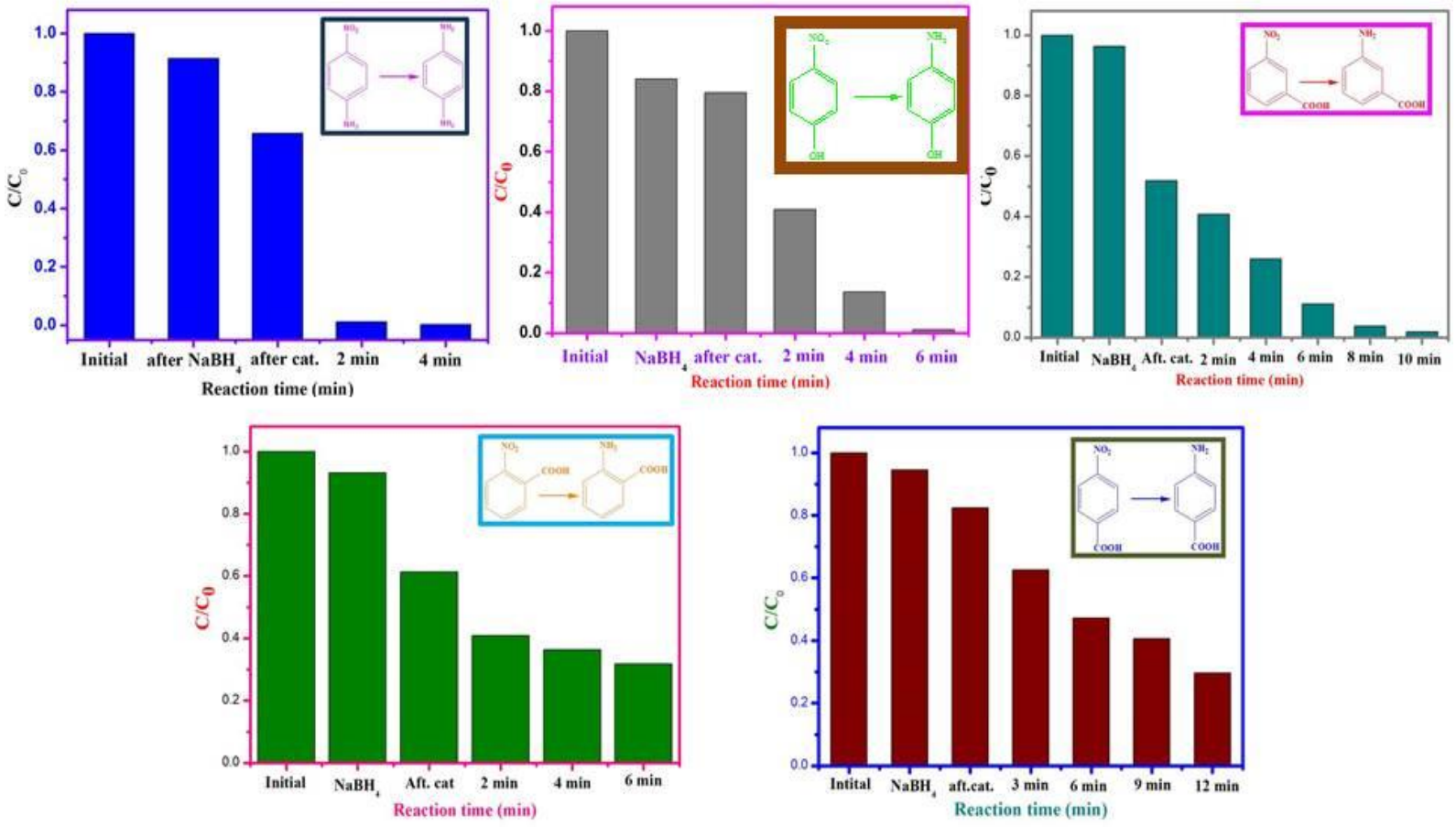

Fig.16. Plot showing the reduction of (a) p-nitroaniline, (b) p-nitrophenol, (c) m-nitrobenzoic acid, (d) o-nitrobenzoic acid and (e) p-nitrobenzoic acid

having various substituent group such as p-nitro aniline, p-nitrophenol, p-nitrobenzoic acid, o-nitrobenzoic acid and m-nitrobenzoic acid. As clearly reflected from the Fig. 17 (a-e), the plots shows the reduction rate of various nitroaromatic compounds after adding sodium borohydride, catalyst and then at regular interval of time. It can be found that the reduction of nitroaniline and

nitrophenol took much lower time to get reduced to p-nitro aniline and p-aminophenol as compared to other nitroaromatic compounds. Since the reduction efficiency is intimately related with the fate and transfer of electron from nitro group to $NaBH_4$, the highly enhanced performance, as observed for photoreduction of aromatic nitro organics, could be attributed to the fact that the addition of Au-Cu bimetallic NPS into the matrix of rGO would remarkably synergistically improve the reduction process of nitroaromatic compounds.

4. Conclusions

Monometallic Au, Cu and bimetallic Au-Cu nanoparticle doped reduced graphene oxide were successfully synthesized using co-reduction method. The UV-Vis study shows the surface e plasmon band for Au and Cu nanoparticles. The XRD Study revealed that the peaks obtained for Au-Cu/rGO are intermediate to the peaks obtained for Au/rGO and Cu/rGO. The FESEM of Au-Cu/rGO confirms the crumbled stacked structure of GO and uniform distribution of bimetallic nanoparticles. The TEM analysis of Au-Cu/rGO confirmed the uniform distribution of bimetallic nanoparticles over reduced graphene oxide sheets with strong interaction between them. The SAED study confirms the crystallinity of the nanocomposites. Later on the reduction of various nitro group compounds were studied using monometallic, bimetallic and the above three types of nanocomposites. It was found that Au-Cu/rGO is the most efficient catalyst above all of the other catalysts. Also, from the comparative study of the catalyst and reducing agent concentration showed that the optimum amount of catalyst was found to be 2 mg and the optimum amount of reducing agent is 0.05 M. Thus, Au –Cu/rGO under optimum concentration of catalyst and reducing agent was found to be a very effective catalyst for the reduction of nitro group compounds.

Chapter 5

Future Work

Monometallic Au, Cu and bimetallic Au-Cu supported reduced graphene oxide has been synthesized so far. The characterization was done using UV-Vis, XRD, FESEM, TEM/SAED, EDS mapping /EDX. The catalytic activity of the catalyst was studied towards the reduction of nitroaromatic compounds. Influences of different parameter such as effect of catalyst dose and concentration of reducing agent have been studied.

Further studies in the group will be the characterization of Au-Cu/rGO catalyst using other sophisticated instrument such as XPS and Raman. XPS study will be useful to know the electronic interaction between nanoparticles and graphene oxide. EDS line scan will be done to confirm the composition of bimetallic nanoparticles. Further we will investigate the influence of temperature on reduction of nitroaromatic compounds. In addition to this catalytic reduction of other nitroaromatic compounds and their kinetic studies will be done in future. All these studies are going on in our lab and one manuscript will be submitted to a chemistry journal soon.

Chapter 6

References

1. R. Grillo, A. H. Rosa and F. L. Fraceto, *Chemosphere*, 2015, **119**, 608-619.
2. R. G. Chaudhuri and S. Paria, *Chem. Rev.*, 2012, **112**, 2373-2433.
3. W. J. Liu, T. T. Qian and H. Jiang, *Chem. Engg. J.* , 2014, **236**, 448-463.
4. C. L. Bracey, P. R. Ellis and G. J. Hutchings, *Chem. Soc. Rev.*, 2009, **38**, 2231-2243.
5. V. K. Gupta, N. Atar , M. Lutfi, Y. Z. Ustundag and L. Uzun, *Water Res.*, 2014, **48**, 210-217.
6. A. Saha and B. Ranu, *J. Org. Chem.*, 2008, **73**, 6867.
7. A. Corma and P. Serna, *Science*, 2006, **313**, 332.
8. N. Sahiner, S. Butun and P. Ilgin, *Colloids Surf. A*, 2011, **386**, 16-24.
9. C. Yu, B. Liu and L. Hu, *J. Org. Chem.*, 2001, **66**, 919-924.
10. A. M. Tafesh and J. Weiguny, *Chem. Rev.*, 1996, **96**, 2035.
11. J. R. Potts, D. R. Dreyer, C. W. Bielawski and R. S. Ruoff, *Polymer* 2011, **52**, 5-25.
12. G. G. Chen, P. Joshi, S. Tadigadapa and P. C. Eklund, *Nano Lett.* , 2006, **6**, 2667.
13. A. Kumar, L. Rout, R. S. Dhaka, S. L. Samal and P. Dash, *RSC Adv.*, 2015, **5**, 39193.
14. D. Chen, H. Feng and J. Li, *Chem. Rev.* , 2012, **112**, 6027-6053.
15. R. Kumar, S. Naqvi, N. Gupta, K. Gaurav, S. Khan, P. Kumar, A. Rana, R. K. Singh, R. Bharadwaj and S. Chand, *RSC Adv.*, 2015, **5**, 35893.
16. K. Ping Loh, Q. Bao, G. Eda and M. Chhowalla, *Nat. Chem.* , 2010, **2**, 1015-1024.
17. D.R. Paul and L. M. Robeson, *Polymer*, 2008, **49**, 3187-3204.
18. R. Wang, Z. Wu, C. Chen, Z. Qin, H. Zhu, G. Wang, H. Wang, C. Wu, W. Dong, W. Fana and J. Wang, *Chem. Commun.*, 2013, **49**, 8250.
19. Z. Huang, H. Zhou, C. Li, F. Zeng, C. Fu and Y. Kuang, *J. Mater. Chem.*, 2012, **22**, 1781.
20. K. Vinodgopal, B. Neppolian, Ian V. Lightcap, Franz Grieser, Muthupandian Ashokkumar and P. V. Kamat, *J. Phys. Chem. Lett.* , 2010, **1**, 1987-1993.

21. X. Liu , X. Wang , P. He , L. Yi , Z. Liu and X. Yi, *J. Solid State Electrochem.*, 2012, **16**, 3929-3937.
22. Y. Hu, P. Wu, H. Zhang and C. Cai, *Electrochimica Acta*, 2012, **85**, 314-321.
23. M. Zahmakıran and S. Özkar, *Nanoscale*, 2011, 3462-3481.
24. X. Liu, D. Wang and Y. Li, *Nano Tod.*, 2012, **7**, 448-466.
25. Q. Shi, R. Lu, L. Lu, X. Fu and D. Zhao, *Adv. Synth. Catal.*, 2007, **349**, 1877.
26. R. J. Rahaim and R. E. Maleczka, *Org. Lett.*, 2005, **7**, 5087.
27. S. Chandrasekhar, S. J. Prakash and C. L. Rao, *J. Org. Chem.* , 2006, **71**, 2196.
28. P. Song, J. Ju Feng, S. X. Zhong, S. Huang, J. R. Chen and A. J. Wang, *RSC Adv.*, 2015, **5**, 35551-35557.
29. P. S. Rathore, R. Patidar, T. Shripathic and S. Thakore, *Catal. Sci. Technol.*, 2015, **5**, 286.
30. C. T. Campbell, J. C. Sharp, Y. X. Yao, E. M. Karp and T. L. Silbaugh, *Faraday Discuss.*, 2011, **152**, 227-239.
31. N. Arul Dhas, C. Paul Raj and A. Gedanken, *Chem. Mater.*, 1998, **10**, 1446-1452.
32. R. Grisel, K. J. Weststrate, A. Gluhoi and B. E. Nieuwenhuys, *Gold Bulletin*, 2002, **35**, 39-45.
33. K. N. Kudin, B. Ozbas, H. C. Schniepp, R. K. Prudhomme, I. A. Aksay and B. Car, *Nano Lett.*, 2008, **8**, 36-41.
34. S. J. Park, J. H. An, R. D. Piner, I. Jung, D. X. Y. A. Velamakanni, S. B. T. Nguyen and R. S. Ruoff, *Chem. Mater.*, 2008, **20**, 6592-6594.
35. Y. Xu, K. Sheng, C. Li and G. Shi, *ACS Nano*, 2010, **4**, 4324-43330.
36. D. Kim, J. Resasco, Y. Yu, A. M. Asiri and P. Yang, *Nat. Comm.*, 2014, **5**, 4948.
37. S. Liu, Z. Sun, Qi. Liu, Li. Wu, Y. Huang, T. Yao, J. Zhang, T. Shripathic, M. Ge, F. Hu, Z. Xie, G. Pan and S. Wei, *ACS*, 2014, **8**, 1886-1892.
38. N. Tian, Z.-Y. Zhou, S.-G. Sun, Y. Ding and L. W. Zhong, *Science*, 2007, **316**, 732-735.
39. S. R. Sahu, M. M. Devi, P. Mukherjee, P. Sen and K. Biswas, *J. Nanomatet.*, 2013, **2013**, 232409-232418.
40. G. Rothenberg, *Catalysis: Concepts and Green Applications*, 2008.
41. S. Saha, A. Pal, S. Kundu, S. Basu and T. Pal, *Langmuir*, 2010, **26**, 2885-2893.